A Neural Network Fault Diagnosis Method applied for Faults in Intake System of an SI Engine

R. Chini
Mechanical Engineering, K.N.Toosi University of Technology, Tehran, Iran
r_chini@sina.kntu.ac.ir

A. H. Shamekhi
Mechanical Engineering, K.N.Toosi University of Technology, Tehran, Iran
shamekhi@kntu.ac.ir

M. H. Behroozi
Iran University of Science and Technology, Tehran, Iran
shamekhi@kntu.ac.ir

M. Mostofi
Mechanical Engineering, University of Mazandaran, Babol, Iran
mehdi_mostofi@yahoo.com

Abstract
One essential part of automated diagnosis systems for SI engines is due to elements of air path system. The diagnosis task is getting more challenging by including Exhaust Gas Recirculation (EGR) which its transient effects on temperament complexity of the air-path system are quite significant. The faults occur in this subsystem can result in deviation in air-fuel ratio, which causes increased emissions, misfire and especially loss of power and drivability problems. In this article, a model-based diagnosis system for air-path of an SI engine with EGR is constructed. In addition, a nonlinear four-state dynamic model of an SI engine with EGR is utilized, and then results are validated by a real engine. In the next step, diagnosis system is designed in the framework of Artificial Neural Network (ANN) classifier. Simulation results show that the constructed diagnosis system for six fault modes considering all three kinds of common faults including actuator, component, and sensor faults is applied successfully. In addition, in this article the Manifold Air Temperature (MAT) sensor fault which comparatively less has been evaluated than other elements are also taken into account.
Keywords: fault diagnosis, mean value modeling, neural network classifier and SI engine.

Introduction

Due to the flexibility and complexity of SI engines the number of potential failure increases and this makes the task of fault diagnosis quite challenging. When faults appear frequently in industrial machinery, the component quality and flexibility of the system will be decreased and consequently the price of manufacturing will be diversely affected.

First serious researches about fault diagnosis of dynamic systems are done in 1970s. Reference [1] in 1971 initiated fault diagnosis based on observers in linear systems. Reference [2] introduced Sensor fault diagnosis for the first time in 1978. Reference [3] in 1991 used Space Relations in diagnosis systems. Reference [4] in 1997, [5] in 1999 and [6] in 2006 accomplished more researches on automotive air path fault diagnosis.

Developing artificial intelligence methods, researches in FDI approaches has been introduced to other levels. Reference [7] in 1986 suggested application of Neural Networks in design of fault diagnostic systems for the first time. In 1997, [8] used Fuzzy logic and Neural Network for estimation of physical parameters of system. More works on applications of Neural Networks in fault diagnosis could be mentioned as [9] in 2004 and [10] in 2006.

In this article, different fault types simulated in inlet system of a modified 1275 cc British Leyland engine has been diagnosed by a Neural Network based diagnostic system. The mathematical model is presented in section 2. In section 3, the characteristics and implementation procedure of faults into the model are demonstrated. The construction of a diagnostic system based on ANN is introduced in section 4, and in the end, the performance quality of proposed diagnosis system is analyzed.

Mathematical Model

Modeling

Here, the mathematical model which is used to study the diagnosis scheme is presented. This model is a nonlinear four state dynamic model of an SI engine with EGR. The model is simulated in SIMULINK toolbox of MATLAB and results are validated with a real engine. Here only the final differential state equations will be shown. Detailed information about this model can be found in [11].

$$\dot{n}=(1-E)\frac{60}{2\pi I_t}\left\{\frac{\eta_{ic} Q_{HV} \dot{m}_f}{\frac{2\pi}{60} n}-\left[a_0+a_1 n+a_2 n^2+(a_3+a_4 n) p_i\right]\right\} \quad (1)$$

$$\dot{m}_{ff}=\frac{1}{\tau_{ff}}\left(-\dot{m}_{ff}+X(1-Y)\dot{m}_{fi}\right) \quad (2)$$

$$\dot{p}_i=\frac{R(1-E)}{V_i}\times\left\{\left[\dot{m}_{at0}+\dot{m}_{at1}\beta_1(\alpha)\beta_2(p_i)\right]T_m-\frac{V_d \eta_v n p_i}{120 R}\right\} \quad (3)$$

$$\dot{T}_i=\frac{R T_i}{p_i V_i}(1-E)\times\left\{\left[\dot{m}_{at0}+\dot{m}_{at1}\beta_1(\alpha)\beta_2(p_i)\right](T_m\kappa-T_i)-\frac{V_d \eta_v n p_i}{120 R}(\kappa-1)\right\} \quad (4)$$

Model Validation

The adiabatic MVEM presented above was compared by experimental results of a 1275 cc British Leyland engine. Differences between engine simulation and measurements can be seen in “Figure 1” to “Figure 4”. Note that notations and descriptions about the parameters and constants used in here are presented in list of symbols at the end of paper.

As it could be seen in "Figure 2", "Figure 3" and "Figure 4", the maximum error is around 5, 8, and 10 percents respectively. It has to be mentioned that the major outcome of the model is its capability in modeling the dynamics of the manifold air temperature which is a crucial factor in diagnosing the MAT sensor faults.

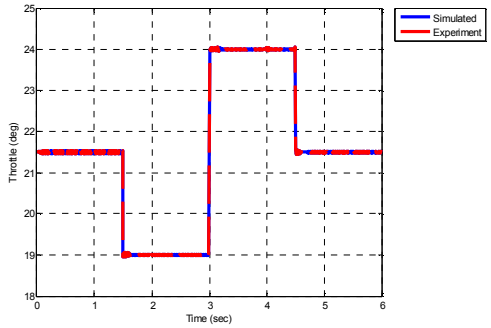

Figure 1: Throttle angle Behaviour through time

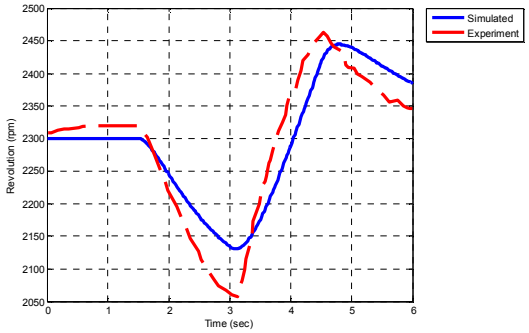

Figure 2: Engine revolution behaviour through time with 10% EGR.

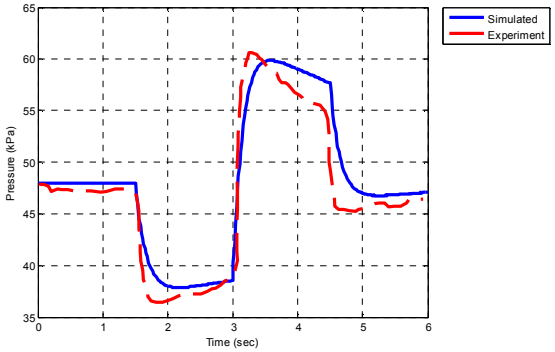

Figure 3: Manifold air pressure behaviour through time with 10% EGR

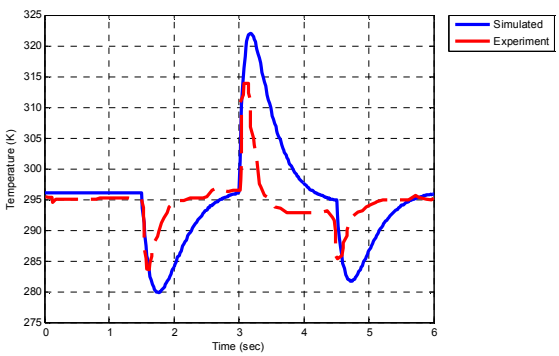

Figure 4: Manifold air temperature behaviour through time with 10% EGR

Modeling of Faults

For the sake of generality, all three types of faults are diagnosed in this paper [5].

No Fault (NF)

In this operational mode, the sensors and actuators are fault free and there is no leakage in the intake system.

Intake manifold Leakage (IL)

For the engine that is used in this work, the intake manifold sub-model pressure during normal operation is always lower than ambient pressure. Hence, a leak in this part is always results in an air flow into the air tube. As a result, faults in this part can not have negative values. The model for IL is obtained by taking the model for NF operational mode, but replacing it with (5). The constraint on the percentage parameter g_{IL}, limited by the performance ranges of modeled SI engine, is $g_{IL} \in [0\ ,15]$.

$$\dot{m}_{at,\,IL} = \dot{m}_{at,\,NF} + g_{IL}\dot{m}_{at,\,NF} \tag{5}$$

Fuel Injector Actuator Gain-Fault (FAG)

In FAG operational mode, the fault is generated in the fuel injector actuator by adding a scalar percentage parameter g_{FAG}. The restriction on g_{FAG} is. $g_{FAG} \in [-8\ ,15]$.

$$\dot{m}_{f,\,FAG} = \dot{m}_{f,\,NF} + g_{FAG}\,\dot{m}_{f,\,NF} \tag{6}$$

Manifold Pressure Sensor Gain-Fault (MPSG)

The model corresponding to this operational mode is related to a gain-fault added to the physical value of the manifold pressure sensor. For implementing the MPSG fault, a gain factor g_{MPSG} is added to (7). The constraint on g_{MPSG} is. $g_{MPSG} \in [-15\ ,15]$.

$$P_{i,\,MPSG} = P_{i,\,NF} + g_{MPSG}P_{i,\,NF} \tag{7}$$

Throttle Actuator Gain-Fault (THAG)

This operational mode is representing a fault in throttle plate actuator. The model of THAG fault has an added parameter g_{THAG}. This parameter range, like other parameters, is limited by the operation ranges of the SI engine model, $g_{THAG} \in [-10\ ,10]$.

$$\alpha_{THAG} = \alpha_{NF} + g_{THAG}\alpha_{NF} \tag{8}$$

Manifold Temperature Sensor Gain-Fault (MTSG)

The MTSG operational mode is modeled as an added gain-fault parameter g_{MTSG} to outcome of MAT sensor. Here, g_{MTSG} is set to $g_{MTSG} \in [-5\ ,15]$ percentage of the manifold temperature values in "no fault" working mode.

$$T_{i,\,MTSG} = T_{i,\,NF} + g_{MTSG}T_{i,\,NF} \tag{9}$$

"Figures 5" and "Figure 6" show effects of above mentioned simulated faults on SI engine model as illustration. The related magnitudes of applied faults, shown in Figures, are listed in "Table 1".

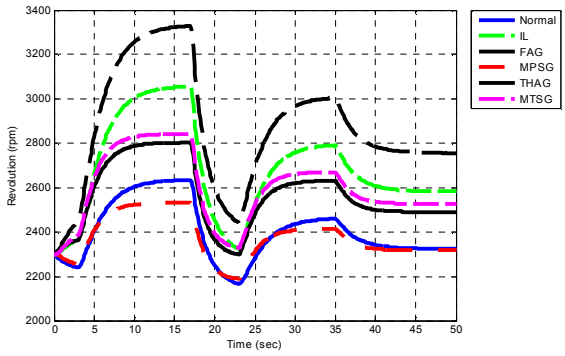

Figure 5: Revolution results of positive fault modeling

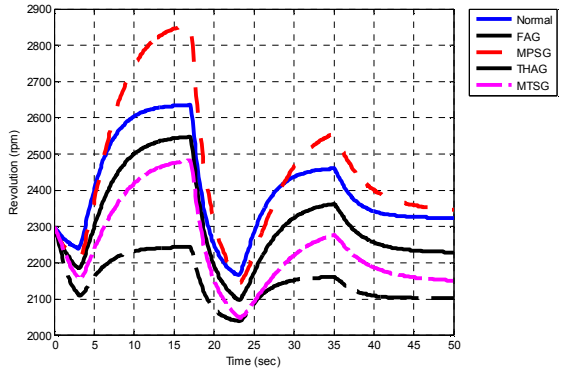

Figure 6: Revolution results of negative fault modeling

Table 1: Faults used as train data

Networks	IL	FAG	MPSG	THAG	MTSG
Positive	10%	10%	7%	6%	7%
Negative	----	-4%	-7%	-6%	-4%

Strategy and Simulation

In this case of study, two distinctive networks are designed and then trained to detect and also isolate pre-defined faults. The first network diagnosis positive ranges of faults and the other one is dedicated to negative counterparts. In this case of study, network inputs are arranged as, engine speed, intake manifold temperature, intake manifold pressure, injected fuel rate, and throttle position. To reduce sensibility to noise and unordered disturbances, it is beneficial to normalize process variables obtained from working conditions of SI engine model in response to above mentioned faults (see "Table 1"). It has to be noted that output signals $y(t)$ and related estimated signals $\overline{y}(t)$ are extracted in each time step of engine performance (0.1 sec).

$$Normalized\ Process\ Variables = \frac{y(t)}{|\overline{y}(t)|} \qquad (11)$$

As it could be seen in "Table 2" and "Table 3", for sorting outputs of each fault mode, a vector with the arrangement of one or zero is selected.

Deviation of real data from ones implemented by the ANN is reported as network errors. These errors are calculated based on mean square error (MSE) formula given below:

$$MSE = \sum_{p=1}^{P}\sum_{i=1}^{N}\left(Y_{real}^{p,i} - Y_{predicted}^{p,i}\right) \qquad (12)$$

Where "i" is number of nodes in output layer, "p" is the number of samples and $Y_{predicted}$ is network outputs and Y_{real} is certified data of SI engine state variables, which extracted before from SI model test procedures.

Table 2: Classification vectors for positive fault classes

NF	IL	FAG	MPSG	THAG	MTSG
1	0	0	0	0	0
0	1	0	0	0	0
0	0	1	0	0	0
0	0	0	1	0	0
0	0	0	0	1	0
0	0	0	0	0	1

Table 3: Classification vectors for negative fault classes

NF	FAG	MPSG	THAG	MTSG
1	0	0	0	0
0	1	0	0	0
0	0	1	0	0
0	0	0	1	0
0	0	0	0	1

Networks are then applied to MATLAB and trained by Quick-propagation ("trainrp" function in MATLAB). Networks are trained surprisingly well with MSE value of 0.0092 for positive network and 0.0081 for negative one. For the purpose of testing the ability of networks for diagnosing the exact trained faults, these faults are fed as inputs to networks. Normalized revolution inputs for both positive and negative network are shown in "Figure 7" and "Figure 8" as examples.

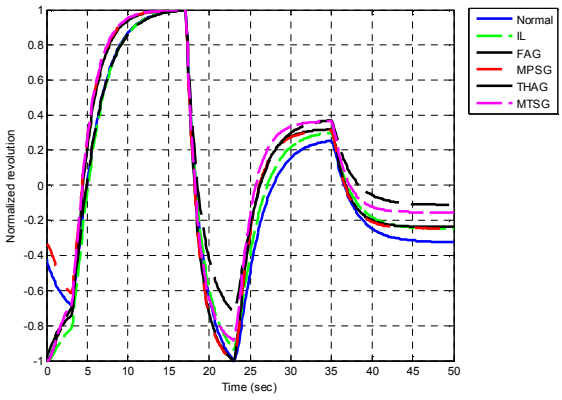

Figure 7: Positive normalized revolution results fed as training input data

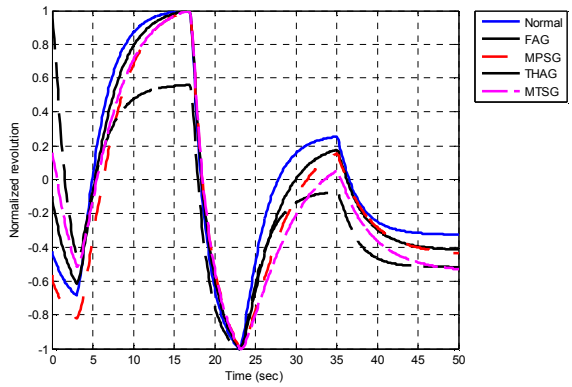

Figure 8: Negative normalized revolution results fed as training input data

It is clear in "Figure 9" and "Figure 10"that networks do exceedingly fine while related fault modes' elements in output vectors are one in almost every 501 samples and remaining fault modes' elements are zero. Some deviations from one and zero are observed, but diagnostic performance of the system is not affected.

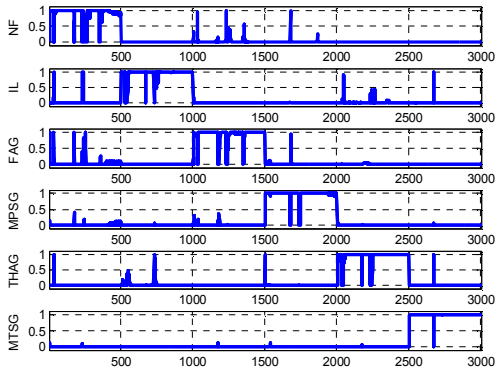

Figure 9: Outputs of positive trained network to its trained faults

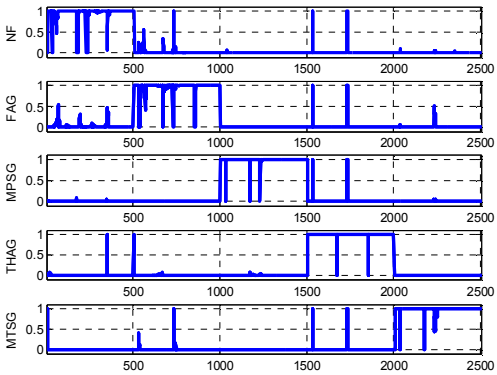

Figure 10: Outputs of negative trained network to its trained faults

To test the generalization and prediction capabilities of networks, different percentages of MPSG fault mode is chosen as input. It has to be noted that MSE values in different fault mode percentages go up when faults deviate from trained data. In this way, if a network enables to isolate a fault mode extreme boundary ranges succesfully, it can isolate entire possible fault mode percentages. Hence, two extreme positive and negative extends of MPSG fault mode were executed on SI engine model and results are fed into networks. In "Figure 11" normalized revolution behavior of MPSG extreme boundaries fed as inputs are shown.

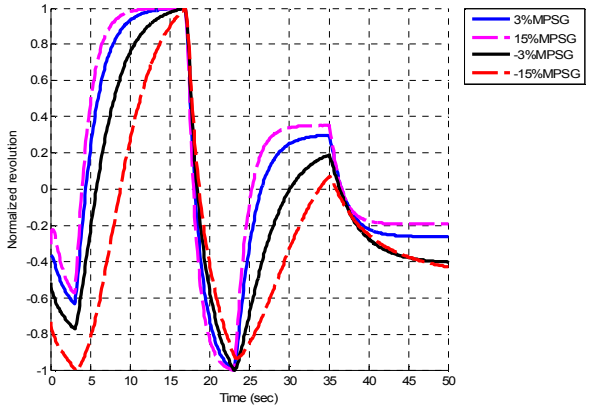

Figure 11: Normalized revolution of MPSG fault mode's boundaries

In order to increase immunity of diagnosis system to small faults and consequently false alarms, the ranges of each fault parameters described in section 3 are extended to (-3,3) for their NF mode in stead of a single value of {0}. In this way, a scalar gain-fault parameter considers as a fault the fault is greater than 3%.

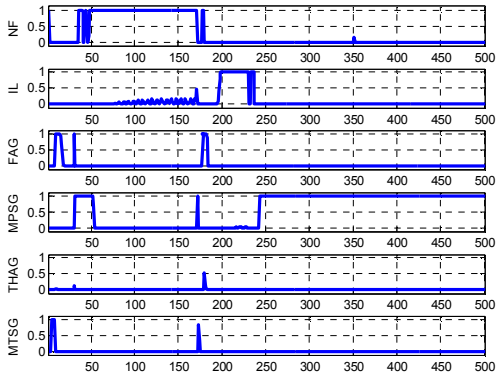

Figure 12: Outputs of the positive neural network to upper positive MPSG ranges

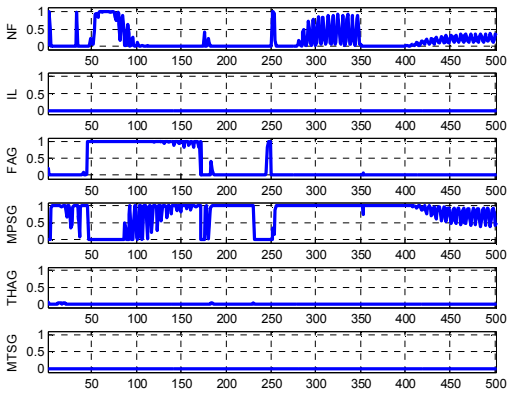

Figure 13: Outputs of the positive neural network to lower positive MPSG ranges

The positive network does well in diagnosis MPSG faults' utmost boundaries. According to "Figure 12" and "Figure 13", it is obvious that IL, THAG, MTSG fault modes are not sensible to positive extensions of this fault mode while they are almost zero in all of their outputs samples. This temperament could be also concluded from "Figure 9" while the positive network has no output other than zero in response to MPSG trained fault in three above mentioned fault modes. In contrast, some deviations from zero are seen in related 501 samples of NF and FAG fault modes of which illustrate their sensibility to MPSG. Moreover, in the first and third row of "Figure 9", there are some oscillations in the fourth part of the samples from 1503 to 2004. These dispositions of samples represent NF and FAG fault modes' dependency to MPSG. These behaviours is somehow degraded the isolation performance of positive network in response to MPSG, NF and FAG fault modes. As it could be seen in "Figure 12", performance of positive network in $g_{MPSG} = 15\%$ case is devalued by this dependency of MPSG and NF fault modes. As a result, some samples are not zero in NF row which is not desirable in isolation MPSG fault mode. It is also understood that FAG fault mode is not sensible to upper positive ranges of MPSG. In $g_{MPSG} = 3\%$ case, the network performance reveals dependency between MPSG, NF and FAG fault modes. As it is clear in "Figure 13", there are some NF and FAG samples which are not zero in response to MPSG lower positive ranges. It is also mentionable that NF fault mode is less sensible than FAG to this boundary of MPSG.

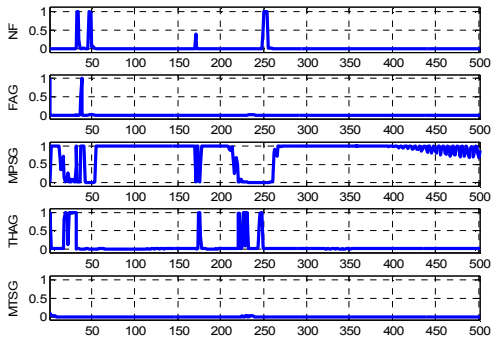

Figure 14: Outputs of the negative neural network to upper negative MPSG ranges

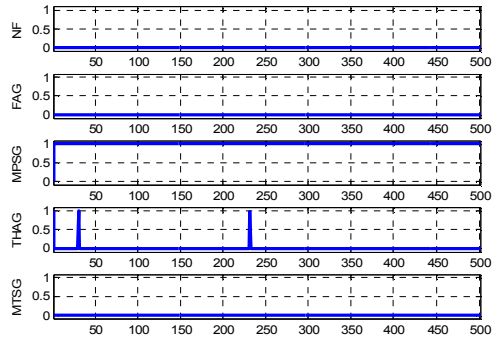

Figure 15: Outputs of the negative neural network to lower positive MPSG ranges

"Figure 14" and "Figure 15" show negative network responses to negative exterme ranges of MPSG. As it is understood from these figures, NF, FAG, THAG and MTSG are completely decoupled from MPSG while their samples are zero in response to MPSG utmost. Although NF and THAG fault mode is rather reacted to MPSG in upper negative ranges, they can be disregarded.

In spite of the fact that sensibility of NF, FAG fault modes to MPSG is worsen the ability of positive network to isolate entire extensions of MPSG fault mode, networks still completely able to fulfill the diagnostic task. In order to certify this fact "Table 4" is provided. In this table, responses of positive and negative networks to all ranges of each fault mode are presented. Networks outcomes are evaluated by integrating the values of each fault mode's samples generated by network, see (13) and (14).

$$P_j^i = [\sum_{n=1}^{501} O_{F,n}] \quad (13)$$

$$N_j^i = [\sum_{n=1}^{501} O_{F,n}] \quad (14)$$

Where "P" and "N" indicate the positive and negative networks' performances, "i" and "j" represent applied fault modes and their percentages respectively. "O" stands for output samples resulted from network for each applied fault modes -which are between 0 and 1- and "F" represents all fault modes that network is capable of diagnose. Finally, "n" is the amount of samples used for representing each fault mode in networks' outputs. Performance indicators "P" and "N" are scalar vectors with six and five members respectively.

Table 4: Responses of networks to all ranges of each fault mode.

	Faults	NF	IL	FAG	MPSG	THAG	MTSG
NF	----	468	0	13	1	0	0
IL	3%	89	236	10	75	0	3
	15%	4	276	1	0	172	2
FAG	-8%	109	----	318	0	151	14
	-3%	133	----	256	0	3	1
	3%	258	0	311	2	1	0
	15%	171	0	254	177	0	0
MPSG	-15%	0	----	0	500	3	0
	-3%	12	----	3	408	27	0
	3%	83	0	131	385	1	0
	15%	137	45	16	282	1	5
THAG	-10%	6	----	12	216	392	0
	-3%	182	----	71	0	272	66
	3%	4	240	1	0	279	2
	10%	16	2	1	0	453	24
MTSG	-5%	8	----	4	1	1	489
	-3%	100	----	19	0	10	383
	3%	0	14	45	1	0	419
	15%	3	0	60	6	4	485

As it could be seen in "Table 4", apart from dependencies among fault modes, the performance values of incident fault mode in both networks are higher than others in all cases. This issue is led to a safe isolation of right fault mode in this diagnosis system while the higher performance factor can correctly isolate the implemented fault mode.
In robustness discussion, presented method is fed by normalized process variables which have an important role in minimizing effects of noises, disturbances and also unordered uncertainties to high degrees. In addition, extending NF operating mode by ignoring small gain-fault parameters was immune the diagnosis system to false alarms. Moreover, as it is discussed above, this method has the ability of diagnosis the whole ranges of faults related to operating conditions of engine. This characteristic empowers this diagnosis system to show robust performance in any working conditions. This method works such an extent that we assert applying this method for real-world engines' fault diagnostic applications.

Conclusions

In this paper, a diagnosis method based on normalized process variable and neural network classifier was developed on intake manifold of an SI engine with EGR. The main goal of this work was to present and apply a diagnostic method which is fast and accurate, and also has low computational cost. For this reason, the diagnosis system was designed by neural network which was shown to be a promising way of diagnosing faults occurred in the intake manifold of the SI engine. This method was capable of diagnosing not only the predefined trained faults, but also entire ranges of these faults. Finally, in spite of the method simplicity, it was completely capable of diagnosing both positive and negative faults with substantially good accuracy and robustness.

Acknowledgments
We are grateful to Dr. S. A. jazayeri from K. N. Toosi University of Technology for helping during the project.

List of symbols

E	EGR ratio
I	Engine moment of inertia (m^4)
$\dot{m}$	Mass flow rate (kg/s)
n	Engine revolution (rpm)
P	Pressure (kPa)
Q	Heating value (kJ)
R	Universal gas constant (mole/kg.K)
T	Temperature (K)
X	Fuel split parameter
v	Volume (m^3)

Greek letters

α	Throttle angle (deg)
η	Efficiency
κ	Gas atomicity coefficient
τ	Time constant coefficient (sec)

Subscripts

a	Ambient
at	past over the throttle plate
d	Displacement
f	Fuel
fc	Fuel conversion
ff	Fuel film
i	Intake manifold
m	Mean
t	Total
v	Volumetric

References

[1] Beard, R., 1971, "Failure Accommodation in Linear systems though self-Reorganization", *Dept. MVT – 71 – 1*, Man Vehicle Laboratory, Cambridge, MA.

[2] Clark, R. N., 1978, "A Simplified Instrument Failure Detection Scheme", *IEEE Transactions Aerospace Electronic System*, **14**, PP: 558-563.

[3] Patton, R. J. and Chen, J., 1991, "Robust Fault Detection Using Eigenstructure Assignment", *a Tutorial Consideration and some New Results, in Proceeding of the 30th IEEE Conference on Decision and Control*, PP: 2242-2247, Brighton.

[4] Nyberg, M. and L. Nielsen, 1997, "Model based diagnosis for the air intake system of the SI-engine", *SAE Paper*, 970209.

[5] Nyberg, M., 1999, *Model Based Fault Diagnosis Methods, Theory, and Automotive Engine Applications*, Ph.D. Thesis, Linkoping, Sweden.

[6] Mostofi, M., Shamekhi, A. H. and Ziabasharhagh, M., 2006, "Developing an algorithm for SI engine diagnosis using parity relations", *Proceedings of IMECE2006, ASME*, IMECE2006-13463, November 5-10, Chicago, Illinois, USA.

[7] Rumelhart, D. E. and McClelland, J. L., 1986, *Parallel Distributed Processing*, MIT Press, Cambridge, Massachusetts.

[8] Frank, P. M. and Seliger, B. K., 1997, "Fuzzy Logic and neural Network Applications to Fault Diagnosis", *International Journal of Approximate Reasoning*, PP. 67-88.

[9] Gen-Ting, Y. and Guang-Fu, M., 2004, "Fault Diagnosis of Diesel Engine Combustion System Based on Neural Network, *Proceedings of the Third International Conference on Machine Learning and Cybernetics*, 26-29 August, Shanghai.

[10] Shen, Y., Cao, L., Wang, Z., Zhou, S. and Gou, B., 2006, "Fault Diagnosis of Diesel Fuel Ejection System Based on Improved WNN", *Proceedings of the 6th World Congress on Intelligent Control and Automation*, June 21 - 23, Dalian, China.

[11] Mostofi, M., Shamekhi, A. H. and Gorji-Bandpy, M., 2006, "Modified Mean Value SI Engine Modeling (EGR Included)", *Proceedings of the International Conference on Modeling and Simulation*, 28 – 30 August, Konya, Turkey.